TMA4212: Chaplygin's equation

C.Elvebakken, E.Johnsen, S.E.Wøllo

October 3, 2019

Abstract

In this project we study Chaplygin's equation, a second order mixed elliptic-hyperbolic equation used in the study of transonic flow; the flow at or near the speed of sound. We mainly study the equation in the subsonic regions, both in terms of the numerical solution with Dirichlet and Neumann conditions and in terms of it's application.

1 Introduction

1.1 Derivation of Chaplygin's Equation

Chaplygin's equation is a second order mixed elliptic-hyperbolic equation on the form

$$u_{xx} + \frac{y^2}{1 - \frac{y^2}{c^2}} u_{yy} + y u_y = 0. \tag{1}$$

When studying an arbitrary steady two-dimensional transonic potential flow, the need for Chaplygin's equation arises from the fact that it is difficult to solve the non-linear equations of motion. The equation describes a transformation which reduces the problem to the solution of a linear partial differential equation [1]. This is done by the hodograph transformation. Below follows a brief derivation of the formula and description of the transformation, which will become useful when studying the application of the equation.

We begin by assuming an isentropic flow without shock waves. By differentiation we see that the velocity potential, ϕ, becomes $d\phi = v_x \, dx + v_y \, dy$. To instead express ϕ in terms of v_x and v_y we use the Legendre transformation to obtain $d\Phi = x \, dv_x + y \, dv_y$, with $\Phi = -\phi + x \, dv_x + y \, dv_y$. We now have the properties $v_x = v \cos \theta$ and $v_y = v \sin \theta$, which again can be given by

$$x = \cos \theta \frac{\partial \Phi}{\partial v} - \frac{\sin \theta}{v} \frac{\partial \Phi}{\partial \theta} \quad \text{and} \quad y = \sin \theta \frac{\partial \Phi}{\partial v} + \frac{\cos \theta}{v} \frac{\partial \Phi}{\partial \theta}. \tag{2}$$

Moreover, to express $\Phi(\theta, v)$, we manipulate the equation of continuity to use the Jacobians instead, and get

$$\frac{\partial(\rho v_x, y)}{\partial(x, y)} - \frac{\partial(\rho v_y, x)}{\partial(x, y)} = 0. \tag{3}$$

By Bernoulli's equation, $w = w_o - \frac{1}{2}v^2$, and knowing that in an isentropic flow the entropy is constant, we can express the density by v. Then, if one substitutes into (3) the new terms for v_x, v_y, x, and y, and a manipulation of Euler's equation of the form $d(\rho v)/dv = \rho(1 - v^2/c^2)$, we obtain Chaplygin's equation on the form

$$\frac{\partial^2 \Phi}{\partial \theta^2} + \frac{v^2}{1 - \frac{v^2}{c^2}} \frac{\partial^2 \Phi}{\partial v^2} + v \frac{\partial \Phi}{\partial v} = 0, \tag{4}$$
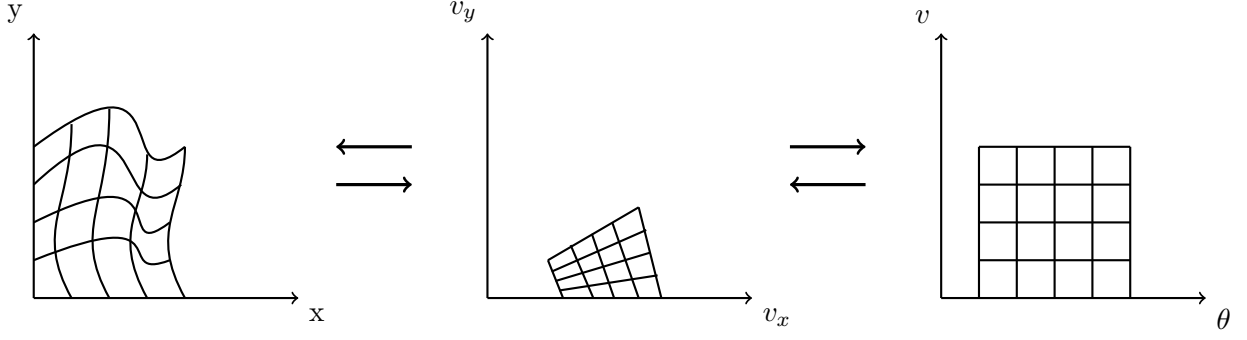
Figure 1: Illustration of arbitrary transformations. Left: physical xy-plane where the motion is non-linear. Center: hodograph plane, in v_x and v_y directions, which shows the velocity components at different positions. Right: Chaplygin plane, in θ and v directions, shows the varying velocity for different angles. Once we have a grid in one of these planes, we can transform it to the others to see different aspects of the transonic flow.

where v is the flow velocity at a given point, c is the velocity of sound, here assumed constant, and θ is the angle of inclination of the velocity. For a more thorough deriving of the equation see §116 in [1].

1.2 Transformation to the Physical Plane

If one wishes to understand the complexity behind potential flow in transonic regions, it could be interesting to map the grid from the $v\theta$-plane, hereby called the Chaplygin plane, to the physical xy-plane. The mappings between the coordinate systems are illustrated in Figure 1.

To define this mapping we begin by recognizing that

$$x = \frac{\partial \Phi}{\partial v_x}, \qquad y = \frac{\partial \Phi}{\partial v_y}, \tag{5}$$

which is a result from the derivation of Chaplygin's equation [1]. As $\Phi = \Phi(\theta, v)$, and is thereby not dependent of v_x and v_y, we can use the chain rule to obtain

$$\frac{d\Phi(v,\theta)}{dv_x} = \frac{\partial \Phi}{\partial v} \cdot \frac{\partial v}{\partial v_x} + \frac{\partial \Phi}{\partial \theta} \cdot \frac{\partial \theta}{\partial v_x}$$
$$\frac{d\Phi(v,\theta)}{dv_y} = \frac{\partial \Phi}{\partial v} \cdot \frac{\partial v}{\partial v_y} + \frac{\partial \Phi}{\partial \theta} \cdot \frac{\partial \theta}{\partial v_y}.$$

This can be written as a linear system of the form

$$\begin{bmatrix} x \\ y \end{bmatrix} = \begin{bmatrix} \frac{\partial v}{\partial v_x} & \frac{\partial \theta}{\partial v_x} \\ \frac{\partial v}{\partial v_y} & \frac{\partial \theta}{\partial v_y} \end{bmatrix} \begin{bmatrix} \frac{\partial \Phi}{\partial v} \\ \frac{\partial \Phi}{\partial \theta} \end{bmatrix} \quad \implies \quad \boldsymbol{X} = A\boldsymbol{b}.$$

As we have no easy way of finding the partial derivative of Φ from the $\boldsymbol{b}$-vector in the inner grid points, we instead approximate these values by central differences to be

$$\frac{\partial \Phi}{\partial v} \approx \frac{\Delta \Phi}{\Delta v} = \frac{\Phi_{i+1,j} - \Phi_{i-1,j}}{v_{i+1,j} - v_{i-1,j}}$$
$$\frac{\partial \Phi}{\partial \theta} \approx \frac{\Delta \Phi}{\Delta \theta} = \frac{\Phi_{i,j+1} - \Phi_{i,j-1}}{\theta_{i,j+1} - \theta_{i,j-1}}.$$

Then, to find the A matrix we use the transformation between the Chaplygin plane and the hodograph plane, given as $v = \sqrt{v_x^2 + v_y^2}$ and $\theta = \arctan(v_y/v_x)$. Differentiating these, we obtain the following matrix

$$\begin{bmatrix} \cos(\theta) & -\frac{1}{v}\sin(\theta) \\ \sin(\theta) & \frac{1}{v}\cos(\theta) \end{bmatrix}.$$

Combining these results, we get the transformation from the Chaplygin plane to the physical plane as

$$\begin{bmatrix} x \\ y \end{bmatrix} = \begin{bmatrix} \cos(\theta_j) & -\frac{1}{v_i}\sin(\theta_j) \\ \sin(\theta_j) & \frac{1}{v_i}\cos(\theta_j) \end{bmatrix} \begin{bmatrix} \frac{\Phi_{i+1,j}-\Phi_{i-1,j}}{v_{i+1,j}-v_{i-1,j}} \\ \frac{\Phi_{i,j+1}-\Phi_{i,j-1}}{\theta_{i,j+1}-\theta_{i,j-1}} \end{bmatrix},$$

where v_i and θ_j are the velocity and angle at a current grid point. This transformation only moves the inner grid points of our original grid, as we cannot use central difference on the boundary points. This could have been avoided by using backward and forward difference along the boundaries. However, we chose not to include the grid points as they wouldn't provide any considerable change to the shape of the transformed grid, which is what we are interested in.

1.3   Defining the Domain

As previously stated, Chaplygin's equation is only valid for transonic flow. That means the equation only describes the motions of objects moving near the speed of sound, c, typically in regions with Mach number around $0.8 - 1.2$ [2]. However, once the object is moving faster than c, shock waves are larger and more frequent. As Chaplygin's equation doesn't take these into account, we must be cautious since not all flows modelled by the equation are therefore physically possible. But, since shock waves are far less prominent at subsonic speeds, we don't accommodate for them numerically, but keep them in mind as a source of error. Another potential pitfall is that the transformation from the Chaplygin plane to the physical plane is not necessarily one-to-one. Therefore, to combat this, one should choose the intervals of v and θ sufficiently small, i.e. $\theta \in (0, \pi/4)$ and $v \in (0.8, 0.9)$. These values are also interesting to look at, since when $v \to c$, the characteristics of transonic flow should be prominent.

The numerical solution of the PDE in the Chaplygin plane is expected to be monotonously increasing, since for higher θ's, we expect higher velocities by Bernoulli's principle [3]. As for the hodograph plane, we presume that the v_y component will vary along with θ, as the fluid changes direction when the angle of displacement increases. However, the v_x component will increase monotonously as θ increases. Lastly, for the physical plane we expect non-linear grid lines, and that they somehow follow the motions of a potential flow.

2   Finite Difference Scheme

2.1   Discretization of the Equation

Chaplygin's equation is classified as an elliptic equation for velocities lower than the speed of sound, the subsonic regions, and a hyperbolic equation for velocities higher than the velocity of sound, the supersonic region. To solve the elliptic equation, we chose to implement a finite difference scheme. For simplicity, we use the notation given in (1) for the derivations of the scheme.

Our scheme for the elliptic equation is made by discretizing the equation with central difference in x- and y-direction for all the three components appearing in the PDE. We assume a square grid at
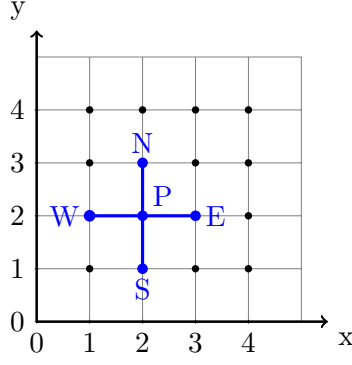
Figure 2: Computational molecule of the five-point formula on a grid. The black points are the inner grid points. The point P is the point we are currently evaluating, and the arms of the molecule, N, W, S, and E, are the contributions from the neighbouring points.

all times, such that the step size in both directions are equal and denoted by h. The discretization of the equation is then given by

$$\frac{1}{h^2}(U_e - 2U_p + U_w) + \frac{\alpha(y)}{h^2}(U_n - 2U_p + U_s) + \frac{y}{2h}(U_n - U_s) = 0,$$

which can be rewritten as

$$\frac{1}{h^2}U_e + \frac{1}{h^2}U_w + \left(\frac{\alpha(y)}{h^2} + \frac{y}{2h}\right)U_n + \left(\frac{\alpha(y)}{h^2} - \frac{y}{2h}\right)U_s - \frac{2(1+\alpha(y))}{h^2}U_p = 0 \qquad (6)$$

where y is the velocity at the point p we are currently at, α is $y^2/(1 - y^2/c^2)$, U_p is the value at the point we are at, and U_e, U_w, U_n and U_s are the values of the points east, west, north and south of p, respectively. This scheme is based on the five-point formula, and it's computational molecule on an arbitrary grid is shown in Figure 2.

By using this scheme we can make a system of equations on the form

$$A\boldsymbol{U} = \boldsymbol{b}$$

where A is a matrix consisting of all contributions from all the points described by (6), $\boldsymbol{U}$ is a vector consisting of all our unknowns, that is the function values for the inner points in our grid, and $\boldsymbol{b}$ is a vector with the boundary conditions corresponding to the correct points. This equation was solved numerically for $\boldsymbol{U}$, which gives us all the unknown function values for our inner grid points.

When implementing this scheme we chose the Dirichlet boundary conditions $u = v\theta$, as this gave us nice plots both in the Chaplygin plane and the physical plane, and seemed to be a reasonable function for the dependency of the velocity and angle.

If we were to use pure Neumann boundary conditions however, we would have to discretize the equation differently. We start by using the five point formula as before, but need to make new schemes for the boundaries of our grid. For the northern boundary we have the condition $u_y|_N = \sigma$. As U_n at this point does not exist, we find a substitution by central difference

$$\sigma = \frac{1}{2h}\left[\left(\frac{\alpha(y)}{h^2} + \frac{y}{2h}\right)U_n - \left(\frac{\alpha(y)}{h^2} - \frac{y}{2h}\right)U_s\right]$$

$$\left(\frac{\alpha(y)}{h^2} + \frac{y}{2h}\right)U_n = \left(\frac{\alpha(y)}{h^2} - \frac{y}{2h}\right)U_s + 2h\sigma.$$

4

By inserting this new value into the five point formula, we get the scheme

$$\frac{1}{h^2}U_e + \frac{1}{h^2}U_w + 2\left(\frac{\alpha(y)}{h^2} - \frac{y}{2h}\right)U_s - \frac{2(1+\alpha(y))}{h^2}U_p = -2h\sigma,$$

which we can use along the northern border. By the same logic we get the schemes

$$\frac{1}{h^2}U_e + \frac{1}{h^2}U_w + 2\left(\frac{\alpha(y)}{h^2} + \frac{y}{2h}\right)U_n - \frac{2(1+\alpha(y))}{h^2}U_p = 2h\sigma$$

$$\frac{2}{h^2}U_w + \left(\frac{\alpha(y)}{h^2} + \frac{y}{2h}\right)U_n + \left(\frac{\alpha(y)}{h^2} - \frac{y}{2h}\right)U_s - \frac{2(1+\alpha(y))}{h^2}U_p = -2h\sigma$$

$$\frac{2}{h^2}U_e + \left(\frac{\alpha(y)}{h^2} + \frac{y}{2h}\right)U_n + \left(\frac{\alpha(y)}{h^2} - \frac{y}{2h}\right)U_s - \frac{2(1+\alpha(y))}{h^2}U_p = 2h\sigma,$$

for the southern, eastern, and western border respectively.

In the numerical implementation we based our Neumann boundary conditions on the properties $\frac{\partial u}{\partial v_x} = x$ and $\frac{\partial u}{\partial v_y} = y$, that are upheld in Chaplygin's equation. To get reasonable plots we chose the boundary condition $u = x + y$ with x ranging from -0.05 to 0, and y from 1.1 to 1.5.

2.2 Convergence of the Scheme

By Lax's equivalence theorem we know that a difference scheme is convergent if and only if it is both consistent and stable. Therefore, we wish to check if our scheme satisfies these criteria.

First, we wish to find the order of our scheme. When discretizing (1), we calculated that

$$\partial^2_{xx} u^n_m = \frac{1}{h^2}\left(U^n_{m+1} - 2U^n_m + U^n_{m-1}\right) + \mathcal{O}(h^2)$$

$$\partial^2_{yy} u^n_m = \frac{1}{h^2}\left(U^{n+1}_m - 2U^n_m + U^{n-1}_m\right) + \mathcal{O}(h^2)$$

$$\partial_y u^n_m = \frac{U^{n+1}_m - U^{n-1}_m}{2h} + \mathcal{O}(h^2),$$

which became the basis of our scheme. We can see that this has order 2, and is also consistent.

To check for stability we rewrite our scheme as

$$U^{n+1}_m = \left(\frac{\alpha}{h^2} + \frac{y}{2h}\right)^{-1}\left[\frac{2(\alpha+1)}{h^2}U^n_m - \left(\frac{\alpha}{h^2} - \frac{y}{2h}\right)U^{n-1}_m - \frac{1}{h^2}\left(U^n_{m+1} + U^n_{m-1}\right)\right], \qquad (7)$$

with $\alpha = y^2/(1 - y^2/c^2)$. By Von Neumann's stability criteria a scheme is stable if there exists a constant $\mu \geq 0$ such that $\xi \leq 1 + \mu h$. We start by requiring $U^{n+1}_m \geq 0$ since we in this project chose to only study areas were this is true. Therefore, we can reformulate our scheme as such

$$\frac{1}{h^2}\left(U^n_{m+1} + U^n_{m-1}\right) \leq \frac{2(\alpha+1)}{h^2}U^n_m - \left(\frac{\alpha}{h^2} - \frac{y}{2h}\right)U^{n-1}_m.$$

We then rewrite U_m^n as $\xi^n e^{i\beta x_m}$, and divide by this term to obtain

$$\frac{1}{h^2}e^{i\beta h} + \frac{1}{h^2}e^{-i\beta h} \leq \frac{2(\alpha+1)}{h^2} - \left(\frac{\alpha}{h^2} - \frac{y}{2h}\right)\xi^{-1}$$

$$\left(\frac{2}{h^2}\cos(\beta h) - \frac{2(\alpha+1)}{h^2}\right)\xi \leq \frac{y}{2h} - \frac{\alpha}{h^2}$$

$$\xi \leq \frac{h}{2}\frac{y/2 - \alpha/h}{\cos(\beta h) - \alpha - 1}$$

$$|\xi| \leq \frac{1}{2}\sqrt{\frac{\alpha^2 - \alpha hy + h^2 y^2/4}{\alpha^2 - 2\alpha\cos(\beta h) + 2\alpha + \cos^2(\beta h) - 2\cos(\beta h) + 1}}.$$

However, as we only look at cases when $y \to c$, the term α^2 tends to infinity and the other components become negligible. We then end up with

$$\sqrt{\frac{\alpha^2}{\alpha^2}} = 1 \leq 1 + \mu h,$$

which means the Von Neumann criteria is fulfilled. Therefore, we can conclude that our method is unconditionally stable when studying transonic motion.
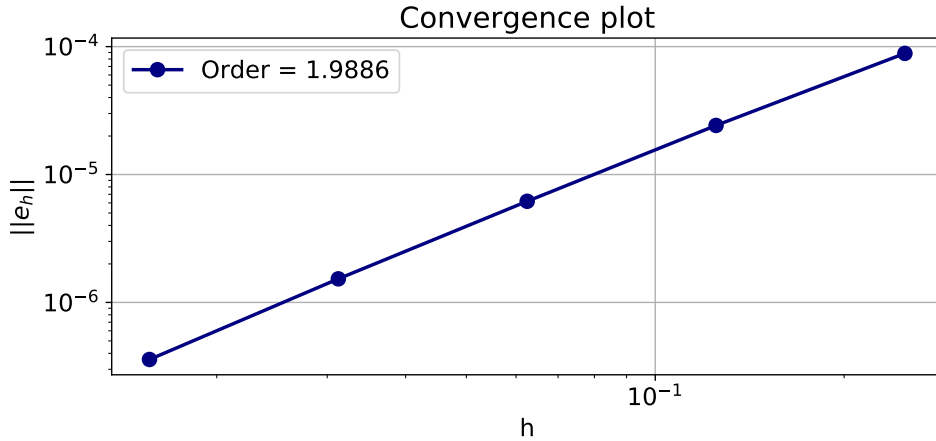

Figure 3: Convergence plot for Chaplygin's equation solved with the five points formula scheme, in subsonic regions with velocities between 0.8 to 0.9 with $\theta = \pi/4$. As the exact solution is not known, this convergence plot was created by comparing the numerical solution with a reference solution with a much smaller step size, specifically $1/220$.

Since we have now shown that our difference scheme is both consistent and stable, we know that it also must converge to the exact solution. This can be seen in the convergence plot in Figure 5. We also see that we obtain order 1.99, which is just as expected.

3   Numerical Results

Solving (4) as an elliptic equation with the discretization described in (6), we obtain the plots shown in Figure 4 and 5. In Figure 4 we have used speeds in the region between 0.8 and 0.9

Mach and $\theta \in [0, \pi/4]$. In Figure 5 we have used the same interval for θ, but with speeds in the range $0.95 - 0.9999$ Mach. We see that for the plots in the Chaplygin plane, the solutions looks almost identical, despite the differing speed intervals. In the hodograph planes, we can see a slight difference in the curling of the graphs, and it looks like the graph straightens out for speeds closer to 1 Mach. The velocities monotonically increase for the higher angles, which is what we expected.
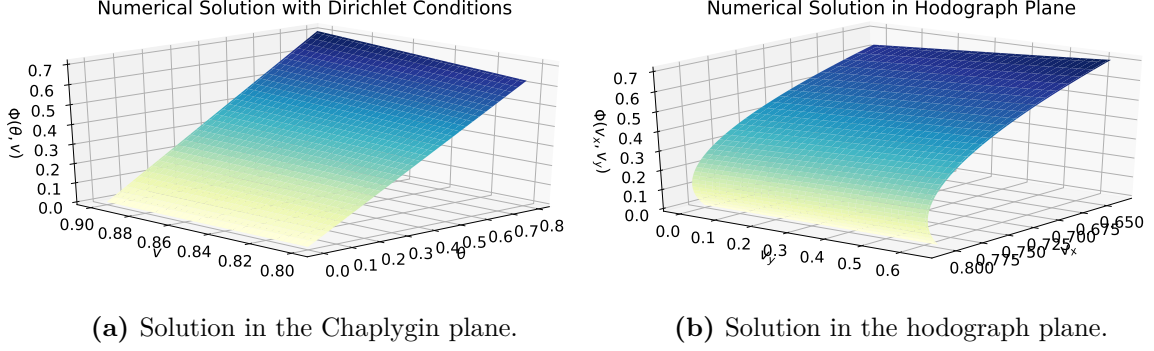

(a) Solution in the Chaplygin plane. **(b)** Solution in the hodograph plane.

Figure 4: Numerical solution of the elliptic equation with Dirichlet boundary conditions. The velocities varies between 0.8 and 0.9 Mach, and θ varies from 0 to $\pi/4$.

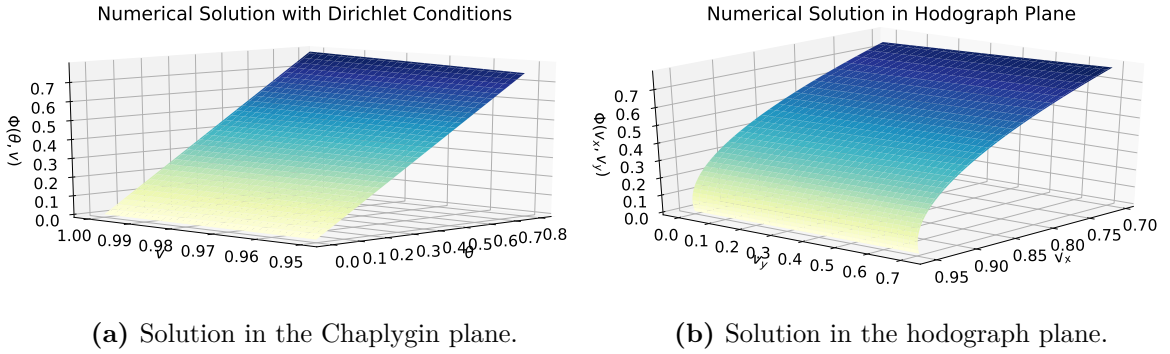**(a)** Solution in the Chaplygin plane. **(b)** Solution in the hodograph plane.

Figure 5: Numerical solution of the elliptic equation with Dirichlet boundary conditions. The velocities varies between 0.95 and 0.9999 Mach, and θ varies from 0 to $\pi/4$.

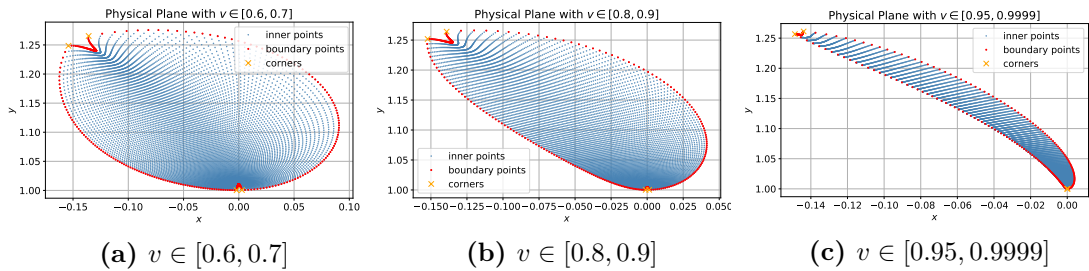**(a)** $v \in [0.6, 0.7]$ **(b)** $v \in [0.8, 0.9]$ **(c)** $v \in [0.95, 0.9999]$

Figure 6: The grid used to solve Chaplygin's equation, plotted in the physical plane, at different velocities.

When transforming our square grid to the physical plane, as discussed in Section 1.2, we get the grids shown in Figure 6. We can see from the complexity of the grid that the motion is non-linear, and much more complicated than what we can see from the graphs in Figure 4 and 5. When varying the velocity intervals, we can see a clear change in the grids, in contrast to the plots in

the Chaplygin plane, which doesn't seem to change much as we approach the speed of sound. The grid becomes more compact for higher speeds, which may be because as the object approaches the speed of sound, the object moves to quickly for the flow to react and spread out.
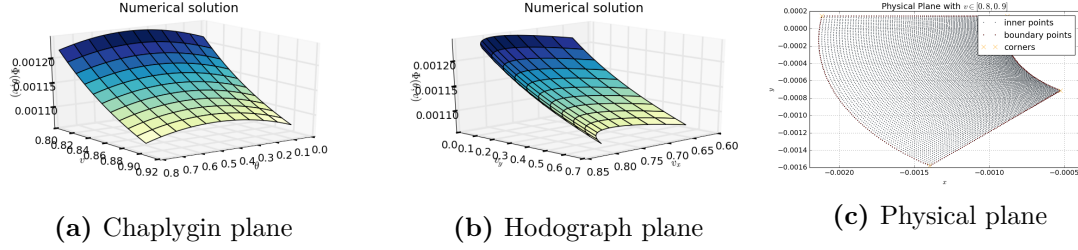

(a) Chaplygin plane   **(b)** Hodograph plane   **(c)** Physical plane

Figure 7: Numerical solutions of the elliptic equation with Neumann boundary conditions.

The solutions of Chaplygin's equation with Neumann boundary conditions are presented in Figure 7. The grid in the physical plane became quite nice as we chose our conditions deliberately to try and get a more normal looking grid, and transform this back into the Chaplygin plane. Though we didn't manage to make a completely square grid, it seems like we somewhat succeeded in making it more regular than in Figure 6.

4   Conclusion

To solve Chaplygin's equation for transonic motion, one can use the five-point formula with either Dirichlet or Neumann boundary conditions. This will give a method that converges to the exact solution of the equation. Chaplygin's equation describes a transformation which reduces the problem to the solution of a linear partial differential equation, using the hodograph transformation. By transforming the grid used to solve the equation back to the physical plane, we can gain a greater understanding of the non-linear nature of the problem we have studied.

In this project, Camilla has implemented a large part of the code, but it terms of the rest of the project, all participants in the group has contributed about equally.

References

[1] L.D.Landau and E.M.Lifshitz. *Fluid Mechanics: Second Edition*. 1987.

[2] Nancy Hall. *Mach Number*. URL: `https://www.grc.nasa.gov/www/k-12/airplane/mach.html`.

[3] *Bernoulli's Principle*. URL: `https://www.nasa.gov/sites/default/files/atoms/files/bernoulli_principle_k-4.pdf`.